A 100 KHZ VIBRATORY MEMS RATE GYROSCOPE WITH EXPERIMENTAL VERIFICATION OF SYSTEM MODEL'S FREQUENCY SCALING

J.-T. Liewald[1], B. Kuhlmann[1], T. Balslink[1] and Y. Manoli[2]
[1]Automotive Electronics, Robert BOSCH GmbH, GERMANY
[2]Fritz Huettinger Chair of Microelectronics, Department of Microsystems Engineering – IMTEK, University of Freiburg, GERMANY

ABSTRACT

The working frequency f_0 of vibratory MEMS angular rate sensors is a main optimization parameter. To investigate the specific challenges of increasing f_0 we designed a new device with f_0=*100 kHz*. Key parameters of the *100 kHz* device are theoretically and experimentally compared with those of a *15 kHz* reference sensor. The experimental results show the validity of the theoretical frequency scaling of the key parameters. The measurements show benefits and disadvantages of MEMS vibratory gyroscopes with increased f_0>>*30 kHz*.

INTRODUCTION

MEMS rate gyroscopes are widely used in automotive and consumer applications. They have continuously been optimized to meet the requirements for modern applications (e.g. Electronic Stability Control systems, image stabilization, dead reckoning, gaming) and to be competitive on the global market.

The working principle of vibratory MEMS angular rate sensors is typically based on the energy transfer from a primary drive oscillation to a secondary sense oscillation due to the Coriolis force [1]. Optimization of MEMS gyroscopes for automotive and consumer applications, is driven by costs, robustness against environmental influences and ease of integration [2]. Since the size of spring mass systems generally decreases with higher resonance frequency the costs in terms of wafer area and the ease of integration are lowered by increasing f_0. Externally applied vibrations can influence the sensor operation, especially if the frequency of the external excitation is near f_0. Thus, the frequency f_0 of the drive oscillation is a main parameter to optimize the vibration robustness of MEMS vibratory rate sensors.

The frequency of published MEMS vibratory gyroscopes today is in the range of *10 to 30 kHz* with only few exceptions (Figure 1). In this frequency range the system behavior corresponds to a mass-spring-damper system with discrete masses and springs. This changes for much higher frequencies (>*1 MHz*) where surface and bulk acoustic waves may be used to measure rotation rate. Today the performance of these gyroscopes does not meet the requirements for modern applications. Therefore we focus on MEMS vibratory gyroscopes [3].

To date, it is not fully investigated which parameters limit the frequency of MEMS gyroscopes and whether frequencies well above *30 kHz* are possible. In this paper we present a prototype of a MEMS gyroscope with f_0=*100 kHz* which is the highest working frequency of published MEMS gyroscopes to date (Figure 1). In order to evaluate the general optimization potential of MEMS gyroscopes with increased f_0, accurate system models are required which can be scaled to the desired frequency. We present measurement results of the new *100 kHz* sensing element which allow an experimental verification of the frequency scaling of key parameters and enable the refinement of current system models.

THEORY

The general system behavior of the micromechanical sensing element is described as a coupled *2nd* order mass spring damper system with linear drive and sense oscillations [1], [4]. Systems with rotational drive or sense oscillation have similar dependencies compared to linear systems.

Key parameters which depend on f_0 are derived from system equations. The most challenging parameters are the drive amplitude $\hat{x}_0$, the drive voltage v_{drive}, the mechanical sensitivity $dy/d\Omega_z$ and the quadrature error Ω_{quad} (Table 1).

Table 1: Key parameters for frequency scaling.

Parameter	Equation	Eqn.-Nr.	Scaling
Drive voltage	$v_{drive} \propto \sqrt{\frac{f_0^2 \hat{x}_0}{Q_{drive}}}$	(1)	↑[a]
drive amplitude	$\hat{x}_{0,\max} \propto \frac{\sigma_{\max}}{f_0^2} \cdot C(f_0)$	(2)	↓
mechanical sensitivity	$\frac{dy}{d\Omega_z} \propto \begin{cases} \hat{x}_0 / f_0 \\ (\hat{x}_0 / f_0) \cdot Q_{sense} \end{cases}$	(3a) (3b)	↓[b] (-)[a,c]
Quadrature error	$\Omega_{quad} \propto \left\lvert \frac{y_{quad}}{\hat{x}_0} \right\rvert \cdot f_0$	(4)	(↑)[c]

$Q_{drive/sense}$: Quality factor of drive/sense oscillator.
$\hat{x}_0$: Nominal drive amplitude.
$C(f_0)$: Geometry term of eq. (2) for different suspension beams.
$\left\lvert \frac{y_{quad}}{\hat{x}_0} \right\rvert$: Mechanical coupling from the drive to the sense oscillation, source of quadrature error. The actual quadrature depends on the specific design (Section Theory/Quadrature signal).

[a]resonant/ [b]off resonant operation [c]design specific

Drive amplitude, drive voltage and mechanical sensitivity

The maximum drive amplitude $\hat{x}_{0,\max}$ is defined by the design of the suspensions and the mechanical strength $\sigma_{\max}$ of the material (e.g. polycrystalline silicon).

The mechanical loads which arise from the drive displacement are proportional to f_0^2. The mechanical resistance for different suspension designs, which is included in the geometry term $C(f_0)$, is proportional f_0 and therefore the maximum drive amplitude $\hat{x}_{0,\max}$ is

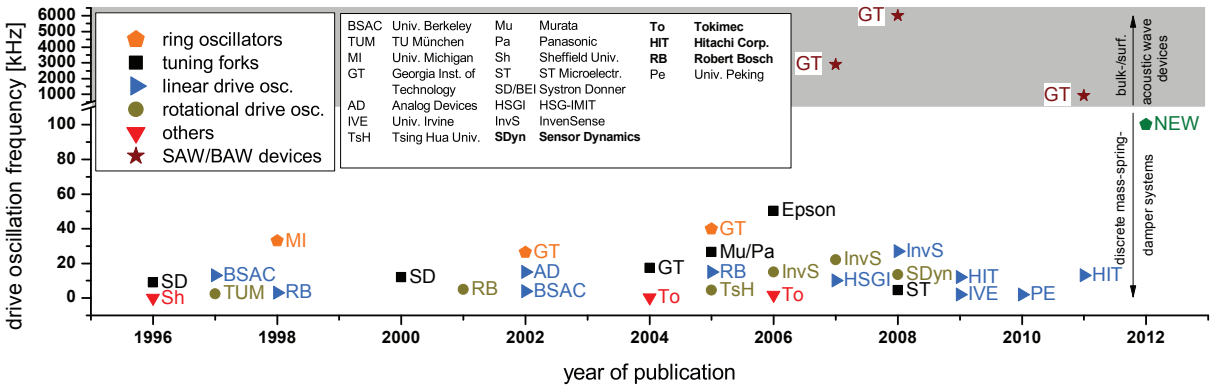

Figure 1: Overview of the working frequency f_0 of published MEMS gyroscopes (selection) comprising separate masses and springs. Surface acoustic wave and bulk wave devices with f_0>1 MHz are included as well. The new 100 kHz element operates within the frequency gap between sensors utilizing discrete springs and masses for signal detection and bulk/surface acoustic wave devices.

proportional to $1/f_0$. This directly reduces the mechanical sensitivity of the sensing element (3) (Table 1) unless the mechanical robustness of the suspension beams can be optimized.

The necessary drive voltage v_{drive} for an oscillation with amplitude $\hat{x}_0$ and resonance frequency f_0 of the drive oscillator decreases if the quality factor Q_{drive} increases. To keep v_{drive} low a drive resonator with low damping and high Q_{drive} is required (1) (Table 1). Q_{drive} is proportional to f_0 for the specific MEMS structures and conditions which are covered in this work. In this case the drive voltage is proportional to $\sqrt{f_0}$ if electrostatic excitation by micromachined comb drives is used. For different actuation principles v_{drive} may rise differently. The maximum possible v_{drive} is limited by the high voltage capability of the ASIC process. The actuation voltage is one parameter which limits the scaling of f_0.

Relation (3a,b) (Table 1) can be derived from the Coriolis force and spring force which act on the detection resonator. $\hat{x}_0$ is limited by geometric, operational and mechanical constraints. For off resonant operation the mechanical sensitivity decreases with frequency (3a) (Table 1). For resonant systems the sensitivity depends on Q_{sense} and therefore on design specific parameters like the mass and the damping of the sense oscillator (3b). With respect to the specific sensor design and resonant or off resonant operation the decrease of mechanical sensitivity may be a limiting factor for increasing f_0.

Quadrature signal

Micromechanical vibratory rate gyroscopes suffer from a mechanical quadrature error [5]. Minute process tolerances and imperfect trench processes lead to imperfect suspensions and to a direct mechanical coupling from the drive to the sense oscillation. The predominant quadrature mechanism depends on whether the drive motion is directed in plane or out of plane. MEMS gyroscopes here are classified as type I, II or III (Table 2) depending on the direction of sense and drive movement.

Minute local process variations [6] are predominant for the quadrature signal of type I gyroscopes. They lead to small, randomly distributed errors of the spring constants k_i of the micromachined bending beams of the suspensions, e.g. due to small variations of the width of the beams. The drive motion gets slightly misaligned which results in the unwanted quadrature displacement. A second quadrature mechanisms is based on imperfect trench processes which generate slightly inclined trench walls [7]. This leads to asymmetric cross sections of the suspension beams and a direct coupling of drive and sense motion even in the case of perfectly matched spring constants k_i [7]. This mechanism is dominant for type II and III gyroscopes.

Structures which have as a first order approximation a constant mechanical coupling $\left|\hat{y}_{quad}/\hat{x}_0\right|$ (eq. (4), Table 1) which does not depend on f_0, have a quadrature error which is proportional to f_0 (eq. (4), Table 1). This is because the quadrature force F_{quad} is proportional to f_0^2 and the Coriolis force F_c is proportional to f_0. The dependence of the quadrature on f_0 may be different if specific design aspects, e.g. the width of the suspension beams, change if the f_0 of a sensor is increased.

The quadrature error of Type II and III gyroscopes typically is in the same range [8]. Type I gyroscopes generally have lower quadrature errors than type II and III. Therefore type I gyroscopes are better suited for higher frequencies due to the lower inherent quadrature error. Nevertheless, the quadrature signal, which is considerably larger than the rate signal even at low frequencies [4], is a limiting factor for increasing the frequency f_0.

Table 2: Quadrature of MEMS vibratory gyroscopes.

Drive	Detection	Type	Quadrature rating
in-plane	in-plane	Type I	low, process variations
in-plane	out-of-plane	Type II	high, trench profiles
out-of-plane	in-plane	Type III	medium-high, trench profiles

100 KHZ SENSING ELEMENT

The experimental investigation is done with a *100 kHz* MEMS gyroscope and, for comparison, a *15 kHz* reference element. The sensor principle of both gyroscopes is type I due to the low inherent quadrature.

The *100 kHz* element consists of two half-structures comprising a (Coriolis-) detection frame with U-shaped suspensions flexible in x and y directions and a drive frame which can only move along the x axis (Figure 2).

The structure is driven by pairs of electrostatic comb drives. With this drive concept the drive motions of the left and right half elements are directed in opposite directions and forces and moments of the drive oscillation sum up to zero.

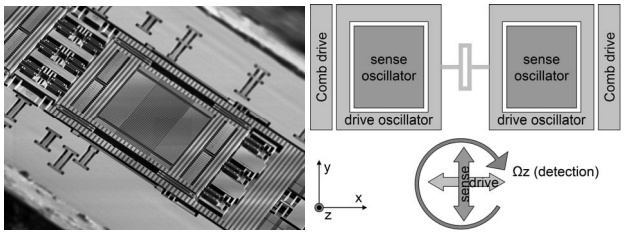

Figure 2: REM picture of the new 100 kHz micromachined sensing element.The schematic drawing illustrates the differential working principle of the newly designed and manufactured prototype.

The elements are processed with the BOSCH surface micromachining process with a functional layer of epitactically deposited polycrystalline silicon [9]. For a better comparison the *15 kHz* reference and the *100 kHz* elements are processed on the same wafer. One challenge of the modal design of the *100 kHz* element arises from the stiffness of the structure in z-direction (out-of-plane). Without additional measures the resonance frequencies of unwanted out-of-plane modes are in the range of *100 kHz*. This particularly results from the quadrature compensation structures. These structures are located within the Coriolis frame and reduce its stiffness. This is compensated for by using a parallel set of suspensions to connect the structure to the substrate at regular distances. In addition the overall dimensions of the structure are *30 %* smaller compared to those of the reference design to increase the overall stiffness of the frame structures. The maximum possible drive amplitude is limited by over travel stops to $1.5 \cdot \hat{x}_0$. The nominal drive amplitude $\hat{x}_0$ is reduced in order to keep the maximum mechanical loads at the suspension beams below the fracture strength σ_{max} of the beams.

The *100 kHz* element has an enhanced electrical sensitivity to face the reduced size of the element which limits the area for detection electrodes and the mass of the sense oscillator. The electrode gaps are *40 %* smaller than those of the reference design. This increases the sensitivity of each single detection electrode by a factor of *1.7* which compensates for the reduced effective area of all detection electrodes and the reduced mass and drive amplitude $\hat{x}_0$. The reduction of the electrode gaps is used to increase the quadrature compensation force as well. The increase of the frequency mainly results from the parallel set of suspensions and the reduced mass of the element. Therefore we assume a quadrature scaling according to (4) (Table 1).

Because of the reduced electrode gaps the squeeze film damping of the sense motion increases and the quality factor Q_{sense} does not linearly increase with f_0. We focus on off resonant signal evaluation which does not directly depend on Q_{sense} but the performance of a resonant system may be lowered because of the increased damping. The (slide film) damping of the drive oscillation remains on the same level due to the shrink of the sensor element and the corresponding quality factor Q_{drive} is proportional to f_0.

EXPERIMENTS

Resonance frequencies

The resonance frequencies f_0 and f_1 of the drive and sense resonators are evaluated with laser vibrometer measurements (Figure 3) and electrical measurements of the amplitude transfer function (Section Theory). For electrical measurements discrete front end electronics and a FPGA are used.

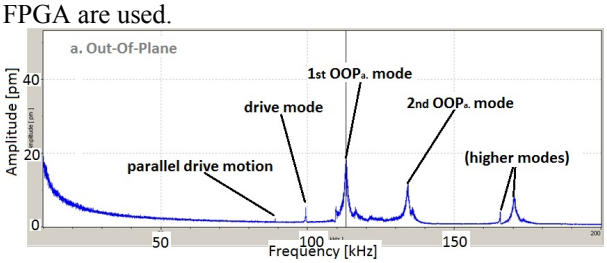

Figure 3: Spectrum of out of plane movements of the new 100 kHz element measured with a laser vibrometer.

Resonant systems are electrically tuned to have $f_0=f_1$ and the range of the unadjusted frequency splitting f_1-f_0 is of interest. The maximum tuning voltage as well as the needed accuracy for frequency tuning influences the ASIC development, e.g. the necessary high voltage capability of the ASIC process or the accuracy of D/A-conversion. In addition it is limited by electrical effects (e.g. snap in voltages, maximum electrical field strength at tuning electrodes). The measurements of f_0, f_1 and f_1-f_0 of the *100 kHz* element are compared with the FE model of the *100 kHz* design. The absolute values and the standard deviations of f_0, f_1 and f_1-f_0 correspond well to the nominal range expected from the FE model and from scaling the corresponding parameters of the *15 kHz* reference elements (Table 3).

Table 3: Drive and sense resonance frequencies.

Parameter (values in Hz)	Estimated/ expected values		*100 kHz* measurements	
	mean value[a]	std. dev.[b]	mean value	std. dev.
f_0 (drive)	101250	500	100500	400
f_1 (detection)	104000	560	103100	600
f_1- f_0 (splitting)	2750	270	3400	170

[a] From FEM simulation.
[b] Reference measurements scaled to *100 kHz*.

Quality factor and sensitivity

A stable drive oscillation is a prerequisite for correct sensor operation. A high quality factor of the drive resonator Q_{drive} is desired to keep the drive voltage v_{drive} low (eq. (1), Table 1). In this work Q_{drive} is derived from the measurement of the amplitude transfer function and the *3 dB* (or half power) bandwidth [10]. The measured values for Q_{drive} are in good agreement with the expected values. The drive voltage which is required to excite a drive oscillation with amplitude $\hat{x}_0$ is also within nominal range.

This is also the case for the mean value of the sensor's sensitivity. The measured value is *15 %* of the reference value which corresponds to the expected scaling (Section *100 kHz* sensing element). The reduced sensitivity lowers the noise performance and hence can be a limiting factor for scaling the frequency of MEMS rate sensors.

Quadrature error

The distribution of the quadrature error of the reference elements is random with respect to the position on the wafer the samples are taken from. This is the same for the measured quadrature errors of the samples of the new element. The random distribution corresponds to the dominant quadrature mechanism of type I gyroscopes (Section Theory → process variations). The mean value and the variation of the measurements are compared to the scaled measurements (according to theory) of the *15 kHz* reference. Figure 4 shows that the absolute quadrature values of the *100 kHz* elements are in the range of the expected values. On average it is *11* times higher compared to the reference element. The variation of the measured quadrature values is *2 to 3* times larger than that of the reference element. Considering the high number of parameters that influence the quadrature of MEMS gyroscopes and with respect to known process variations the difference between theoretical and experimental values is within a reasonable range (Section Theory).

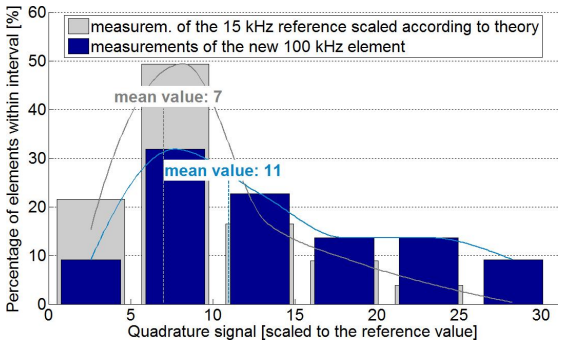

Figure 4: Historgam of the quadrature values of the manufactured 100 kHz elements and of the reference sensors (scaled according to theory). The measured quadrature value of the new element is slightly higher than the expected value.

SUMMARY

New prototypes of *100 kHz* vibratory MEMS gyroscope were designed and manufactured. The elements are fully functional and allow an experimental characterization. The experimental results show that the key parameters of the new element can be estimated from the *15 kHz* reference model if the model is scaled to *100 kHz*. In addition they show that the parameter variations scale as well. This information may be used to estimate the requirements for the evaluation circuit (e.g. voltage capabilities, accuracy for frequency adjustment).

Measurements show, that the absolute quadrature values rise more than proportional to the sensor's working frequency. The high quadrature values require high voltages for quadrature compensation which may exceed electrical or process limits (e.g. maximum voltage of the ASIC process, snap in voltage, maximum electrical field strength). Type II and III gyroscopes (Table 2) typically have even higher quadrature errors. The quadrature error is the limiting factor for increasing the working frequency of MEMS based gyroscopes.

One of the benefits of increasing f_0 is the reduced size of the sensing element. This simplifies the integration and, in terms of wafer area, reduces the costs.

CONCLUSION

In this paper the key parameters (drive voltage and amplitude, sensitivity and quadrature error) for increasing the frequency of a MEMS vibratory gyroscope are theoretically and experimentally investigated. For the first time we present a working *100 kHz* MEMS vibratory gyroscope which is fabricated with the BOSCH process. The elements are fully functional and allow an electrical and optical characterization. Theory and measurement results show that the quadrature error is one of the most challenging parameters for increasing f_0. The experimental characterization of the new sense element verifies the scaling of key parameters derived from a *15 kHz* reference model.

REFERENCES

[1] F. Ayazi, M. F. Zaman, and A. Sharma, "Vibrating gyroscopes," in Comprehensive Microsystems, Y. Gianchandani, O. Tabata and H. Zappe, Eds. Oxford: Elsevier, 2008, pp. 181 – 208.

[2] R. Neul, U.-M. Gomez, K. Kehr, W. Bauer, J. Classen, C. Döring, E. Esch, S. Gotz, J. Hauer, B. Kuhlmann, C. Lang, M. Veith and R. Willig, "Micromachined angular rate sensors for automotive applications," IEEE Sensors J., vol. 7, no. 2, pp. 302–309, 2007.

[3] W. K. Sung, M. Dalal, and F. Ayazi, "A mode-matched 0.9 mhz single proof-mass dual-axis gyroscope," in Proc. 16th Int. Solid-State Sensors, Actuators and Microsystems Conf. (TRANSDUCERS), 2011, pp. 2821–2824.

[4] M. Saukoski, L. Aaltonen, and K. A. I. Halonen, "Zero-rate output and quadrature compensation in vibratory mems gyroscopes," IEEE Sensors J., vol. 7, no. 12, pp. 1639–1652, 2007.

[5] M. S. Weinberg and A. Kourepenis, "Error sources in in-plane silicon tuning-fork mems gyroscopes," J. Microelectromech. Syst., vol. 15, no. 3, pp. 479–491, 2006.

[6] A. S. Phani, A. A. Seshia, M. Palaniapan, R. T. Howe, and J. A. Yasaitis, "Modal coupling in micromechanical vibratory rate gyroscopes," IEEE Sensors J., vol. 6, no. 5, pp. 1144–1152, 2006.

[7] P. Merz, W. Pilz, F. Senger, K. Reimer, M. Grouchko, T. Pandhumsoporn, W. Bosch, A. Cofer, and S. Lassig, "Impact of si drie on vibratory mems gyroscope performance," in Proc. Int. Solid-State Sensors, Actuators and Microsystems Conf. TRANSDUCERS 2007, 2007, pp. 1187–1190.

[8] M. Traechtler, T. Link, J. Dehnert, J. Auber, P. Nommensen, and Y. Manoli, "Novel 3-axis gyroscope on a single chip using soitechnology," in Proc. IEEE Sensors, 2007, pp. 124–127.

[9] M. Offenberg, F. Lärmer, B. Elsner, H. Münzel, and W. Riethmüller, "Novel process for a monolithic integrated accelerometer," in Proc. and Eurosensors IX. Solid-State Sensors and Actuators Transducers '95. The 8th Int. Conf, vol. 1, 1995, pp. 589–592.

[10] W. O. Davis, "Measuring quality factor from a nonlinear frequency response with jump discontinuities," J. Microelectromech. Syst., vol. 20, no. 4, pp. 968–975, 2011.

CONTACT

*J.-T. Liewald, tel. +49(7121)35-39069;
timo.liewald@de.bosch.com